Parametric fluorescence and second-harmonic generation in a planar Fabry-Perot microcavity

Andrea Aiello*
Dipartimento di Fisica, Università degli Studi di Roma, ''La Sapienza,'' Piazzale Aldo Moro 2, 00185 Rome, Italy

Daniele Fargion†
Dipartimento di Fisica and INFN, Università degli Studi di Roma, ''La Sapienza,'' Piazzale Aldo Moro 2, 00185 Rome, Italy and Faculty of Engineering, Technion Institute, Haifa, Israel

Elena Cianci‡

(Received 10 October 1997; revised manuscript received 2 April 1998)

In this work we develop a quantum theory of second-order nonlinear optical processes such as parametric fluorescence and second-harmonic generation (SHG), generated by a strong electromagnetic field in an active medium placed in a microcavity. Fields are quantized and expanded in terms of a suitable set of cavity normal modes. In the first part of this work we consider a single many-level quantum system (an atom or molecule), which interacts with all the radiation field modes (spontaneous emission). We show how vacuum fluctuations affect both SHG and parametric processes. For SHG, we demonstrate that the presence of the microcavity allows the introduction of the concept of coherence length, even for a medium made of a single molecule. In the second part of this paper we discuss the case of a uniform distribution of emitting dipoles. For this configuration we calculate the differential extinction coefficient, and discuss the dependence of the emitting power on the microcavity's parameters. Finally we suggest the possibility of realizing a micro-optical parametric oscillator. [S1050-2947(98)03008-X]

PACS number(s): 42.55.Sa, 42.65.−k, 42.65.Ky, 42.65.Yj

I. INTRODUCTION

Since the second half of the 1980s, questions about cavity QED have attracted the interest of many scientists [1]. In particular, problems regarding the confinement of the electromagnetic field in microscopic structures (microcavities) have turned out to be among the most interesting ones in contemporary physics [2]. Matters concerning spontaneous emission (SpE) from a single atom have been studied extensively [3,4] by means of theories that, beginning from a unidimensional model of the cavity, developed to include the description of the emitted field distribution outside the cavity [5–7]. Moreover, lasers working in microcavities (microlasers), in which the active medium is made of organic molecules diluted in a proper solvent [8,9], or of semiconductor materials [3], have been subjects of theoretical and experimental research. In such a wide research field there are relatively few works regarding nonlinear optical processes in a microcavity [10,11]. With this work we intend to start a systematic investigation of these processes, beginning from the parametric fluorescence and the second-harmonic generation (SHG).

Parametric fluorescence and SHG are among the most important nonlinear optical processes which involve three photons [12]. Such processes can be divided into two classes: in the first class there are those processes in which one photon is annihilated and two are created (parametric interactions); to the second class belong those processes in which two photons are annihilated and one is created (SHG). However, the quantum state of the nonlinear medium does not change in either category of processes, and can thus be considered as belonging to a unique class of elastic scattering of light, and can be described using a homogeneous formalism [13,14]. It is possible to characterize these processes by their differential cross sections if we treat scattering events from isolated molecules, or by their differential extinction coefficient if we consider scattering from a dense medium. Actually both formulations end with a calculation of the process scattering amplitude, which depends on the physical features of the nonlinear medium and on the mode structure of the electromagnetic field surrounding the scattering system. We show how this structure can be modified by the confinement of the field inside a planar microcavity, and how such alterations affect the nonlinear processes. This paper is organized as follows. In Sec. II, we first introduce the traveling wave modes of the cavity, and then the radiation field is quantized in terms of these modes. Then we calculate the interaction Hamiltonian in a microcavity and expand it perturbatively. In Sec. III, we calculate the transition probability both for parametric processes and for SHG. In Sec. IV, we examine the effect of the cavity on vacuum fluctuations; then, in Sec. V, we investigate their effects on SHG emission by a single molecule, and find a similarity with the emission by a finite crystal in free space. In Sec. VI, we calculate the differential extinction coefficient for a dense medium inside a microcavity. Finally, we summarize our results in Sec. VII.

II. FIELD QUANTIZATION AND THE INTERACTION HAMILTONIAN

We consider a cavity made of plane parallel mirrors, such as a Fabry-Perot mirror. For simplicity we assume the mir-

*Electronic address: andrea.aiello@roma1.infn.it
†Electronic address: daniele.fargion@roma1.infn.it
‡Electronic address: cianci@amaldi.fis.uniroma3.it

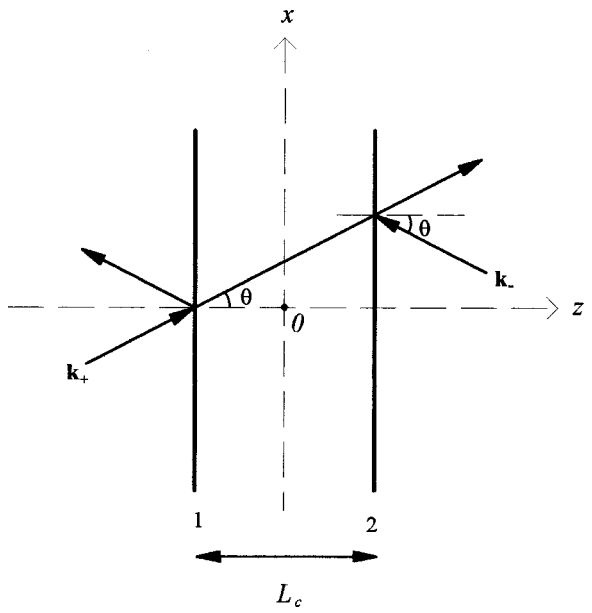

FIG. 1. Scheme of the microcavity model, showing the directions of the two kinds of modes of wave vectors $\vec{k}_+$ and $\vec{k}_-$. L_c is the distance between mirrors labeled with indexes 1 and 2.

rors to be ideal, i.e., with no thickness and absorption. We also consider infinitely extended mirrors in order to avoid complications arising from diffraction from edges. Several authors have found the forms of normal modes in the cavity; we adopt the model introduced by De Martini *et al.* [15]. The cavity geometrical arrangement is shown in Fig. 1. The origin of the coordinates is midway between the two mirrors, which are labeled 1 and 2. The distance between them is L_c, and the z-axis direction is perpendicular to the external surface of mirror 2. Details of calculations are reported in Refs. [15,16]. Here we use slightly different notations than those adopted in Ref. [15], and we introduce a quantization volume V.

The cavity optical features are specified by the reflection and transmission coefficients denoted by r_{1s}, t_{1s} and r_{2s}, t_{2s} for mirrors 1 and 2, respectively. The lowest index $s=1$ and 2 denotes the polarization. For every direction (θ,ϕ) and polarization s, it is possible to construct two sets of mode functions inside the cavity $(-L_c/2 \leqslant z \leqslant +L_c/2)$ by summing the geometrical series resulting from the multiple reflections at the mirrors:

$$\vec{L}_{\vec{k}s}(\vec{x}) = \vec{\epsilon}_{\vec{k}_+ s} \frac{t_{1s}}{D_s} \exp(i\vec{k}_+ \cdot \vec{x}) + \vec{\epsilon}_{\vec{k}_- s} \frac{t_{1s} r_{2s}}{D_s} \times \exp(i\vec{k}_- \cdot \vec{x} + ikL_c \cos\theta), \quad (1)$$

$$\vec{R}_{\vec{k}s}(\vec{x}) = \vec{\epsilon}_{\vec{k}_- s} \frac{t_{2s}}{D_s} \exp(i\vec{k}_- \cdot \vec{x}) + \vec{\epsilon}_{\vec{k}_+ s} \frac{t_{2s} r_{1s}}{D_s} \times \exp(i\vec{k}_+ \cdot \vec{x} + ikL_c \cos\theta), \quad (2)$$

where

$$D_s \equiv 1 - r_{1s} r_{2s} \exp(2ikL_c \cos\theta). \quad (3)$$

These mode functions satisfy the following relations of ortonormality:

$$\int_V d^3x \vec{F}_{\vec{k}s}(\vec{x}) \cdot \vec{G}^*_{\vec{k}'s'}(\vec{x}) = 2\pi V \delta_{FG} \delta_{\vec{k}\vec{k}'} \delta_{ss'}, \quad (4)$$

where F and G stand for L or R. These mode functions, jointly with other mode functions introduced in Ref. [15], form a complete set that couples the interior space with the outside space of the cavity.

Now we consider the interaction of a many-level quantum system placed inside a microcavity with an electromagnetic field. The field can be quantized in the usual way [17], provided that the expansion in terms of plane waves, which holds in the free space, is replaced by the expansion in terms of the mode functions described previously. It is convenient to divide the expression of the electromagnetic field into two parts with opposite parity with respect to the x-y plane:

$$\hat{\vec{E}}_{\rm cav}(\vec{x},t) = \hat{\vec{E}}^{(L)}(\vec{x},t) + \hat{\vec{E}}^{(R)}(\vec{x},t), \quad (5)$$

where we put

$$\hat{\vec{E}}^{(F)}(\vec{x},t) = \sum_{\vec{k},s} i \left(\frac{\hbar c k}{2\epsilon_0 V} \right)^{1/2} \vec{F}_{\vec{k}s}(\vec{x}) \hat{a}^{(F)}_{\vec{k}s} e^{-ickt} + \text{H.c.} \quad (F=L,R). \quad (6)$$

The field operators $\hat{a}^{(L)}_{\vec{k}s}$ and $\hat{a}^{(R)}_{\vec{k}s}$ satisfy the usual commutation rules:

$$[\hat{a}^{(F)}_{\vec{k}s}, \hat{a}^{(G)\dagger}_{\vec{k}'s'}] = \delta_{FG} \delta_{\vec{k}\vec{k}'} \delta_{ss'}, \quad (F=L,R;\ G=L,R). \quad (7)$$

The total Hamiltonian, free part plus interaction term, is the same as in Ref. [15]. The nonlinear processes we analyze involve three photons, but the electric dipole interaction operator has nonzero matrix elements only for those transitions where the number of field photons changes by one. Thus the parametric diffusion and other three-photon processes are just present in the third-order perturbation theory. The first nonvanishing term can be written as

$$\hat{U}^{(3)}_I(t,-\infty) = \left(\frac{-ie}{\hbar} \right)^3 \int_{-\infty}^{t} dt_1 \int_{-\infty}^{t_1} dt_2 \int_{-\infty}^{t_2} dt_3 \times \sum_{m,n,l,r} |m\rangle\langle r| e^{i\omega_{mn} t_1} e^{i\omega_{nl} t_2} e^{i\omega_{lr} t_3} \times [\hat{\vec{D}}_{mn} \cdot \hat{\vec{E}}_{\rm cav}(t_1)][\hat{\vec{D}}_{nl} \cdot \hat{\vec{E}}_{\rm cav}(t_2)] \times [\hat{\vec{D}}_{lr} \cdot \hat{\vec{E}}_{\rm cav}(t_3)], \quad (8)$$

where $\hbar\omega_{ab} \equiv E_a - E_b$ is the difference between system energy levels $|a\rangle$ and $|b\rangle$, and $\hat{\vec{D}}_{ab} \equiv \langle a|\hat{\vec{D}}|b\rangle$ are the matrix elements of its dipole moment $-e\hat{\vec{D}}$. If we expand expression (8), we obtain four kinds of terms: the first two, whose forms are $\hat{a}\hat{a}\hat{a}$ and $\hat{a}^\dagger\hat{a}^\dagger\hat{a}^\dagger$, represent the three-photon absorption and emission, respectively. They are forbidden by

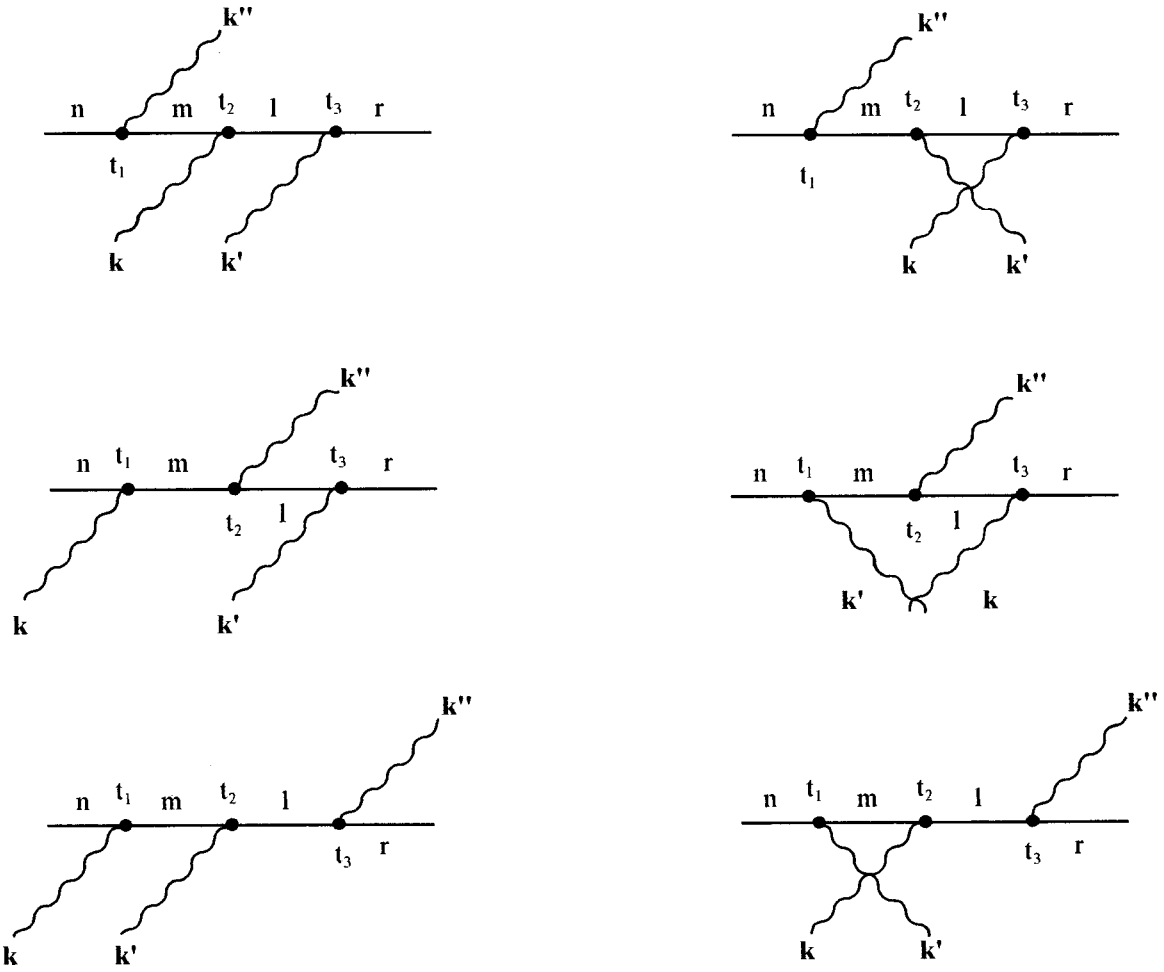

FIG. 2. Diagrammatic representation of the six contributions to parametric fluorescence in third-order time-dependent perturbation theory. All six interactions in each diagram occur via an electric-dipole Hamiltonian.

the energy conservation requirement in the elastic-scattering events we are studying. Then there are terms such as $\hat{a}^{\dagger}\hat{a}\hat{a}$, which are responsible for sum frequency generation (SFG) and SHG processes, and terms such as $\hat{a}^{\dagger}\hat{a}^{\dagger}\hat{a}$ which generate parametric processes. In Eq. (8) there are six terms for SFG and six for parametric fluorescence represented by Feynman diagrams in Fig. 2. It is worthwhile noting that every diagram corresponds to a single term in the expression of the coherent scattering tensor that will be introduced in Sec. III. This tensor satisfies Kleinman's conjecture [12]; indeed, the symmetry-imposed restrictions on the number of independent d_{ijk} elements apply when nonlinear polarization is of electronic origin, as in this case.

III. DERIVATION OF TRANSITION PROBABILITY

A. Parametric processes

Let us consider parametric fluorescence processes. The geometrical arrangement is shown in Fig. 3: L_c is the cavity length, and L_x and L_y are the transverse dimensions of the pump beam; the molecule with dipole moment $-e\vec{D}$ is at $\vec{x}$ inside the cavity. The initial state of our system, that is the many-level quantum system (that we assume to be a molecule) and the electromagnetic field, is represented by

$$|\psi_i\rangle = |g\rangle_M \otimes |\phi_P\rangle_F \equiv |g, \phi_P\rangle, \tag{9}$$

where the molecule is in its ground state $|g\rangle_M$, and we assume the radiation field is in a coherent state $|\phi_P\rangle_F$ with wave vector $\vec{k}_P$ and polarization direction $\hat{x}$; so we write

$$|\phi_P\rangle_F = \exp\left(-\frac{1}{2}|\alpha_P|^2\right)\sum_{N_P}\frac{\alpha_P^{N_P}}{\sqrt{N_P!}}|N_P\rangle_F . \tag{10}$$

The final molecular state is still the ground state, while the radiation field can be in four different final states because of the presence of the cavity:

$$\begin{aligned}
|\phi_1\rangle_F &= \hat{a}^{(L)\dagger}_{\vec{k}_1 s_1}\hat{a}^{(L)\dagger}_{\vec{k}_2 s_2}|0\rangle_F|N_P-1\rangle_F,\\
|\phi_2\rangle_F &= \hat{a}^{(R)\dagger}_{\vec{k}_1 s_1}\hat{a}^{(R)\dagger}_{\vec{k}_2 s_2}|0\rangle_F|N_P-1\rangle_F,\\
|\phi_3\rangle_F &= \hat{a}^{(L)\dagger}_{\vec{k}_1 s_1}\hat{a}^{(R)\dagger}_{\vec{k}_2 s_2}|0\rangle_F|N_P-1\rangle_F\\
|\phi_4\rangle_F &= \hat{a}^{(R)\dagger}_{\vec{k}_1 s_1}\hat{a}^{(L)\dagger}_{\vec{k}_2 s_2}|0\rangle_F|N_P-1\rangle_F .
\end{aligned} \tag{11}$$

We can now calculate the transition rate W [17],

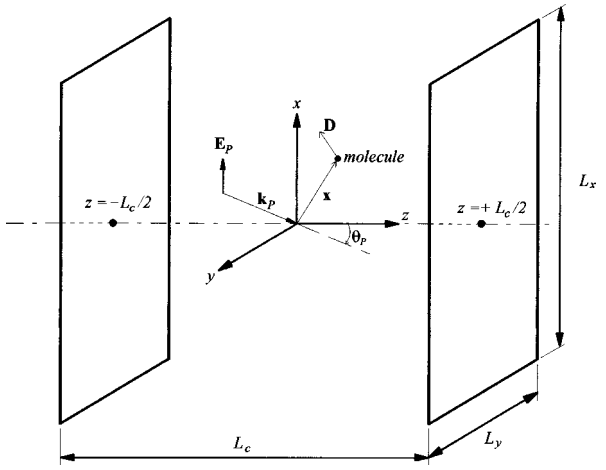

FIG. 3. Geometry of the cavity showing the position of the dipole $\vec{D}$ and the incident pump beam of the wave vector $\vec{k}_P$. L_c is the cavity length, and L_x and L_y are the smallest transverse dimensions between the mirrors and the pump beam sizes.

$$
\begin{aligned}
W &= \frac{|(\psi_f, \hat{U}_I^{(3)}(t,-\infty)\psi_i)|^2}{T} \\
&= \frac{1}{T}\sum_{f=1}^{4}\sum_{N_P}\left|\exp\left(-\frac{1}{2}|\alpha_P|^2\right)\right. \\
&\quad \left.\times\frac{\alpha_P^{N_P}}{\sqrt{N_P!}}\langle g,\phi_f|\hat{U}_I^{(3)}(t,-\infty)|g,N_P\rangle\right|^2 \\
&= \sum_{f=1}^{4}\overline{N}_P\,\frac{2\pi\omega_1\omega_2\omega_P}{\hbar^3}\left(\frac{e^2}{2\epsilon_0 V}\right)^3|\mathcal{M}_f|^2\delta(\omega_P-\omega_1-\omega_2),
\end{aligned}
\tag{12}
$$

where $\overline{N}_P=|\alpha_P|^2$ and the scattering amplitude $\mathcal{M}_f$, evaluated for example for $f=1$, is

$$
\begin{aligned}
\mathcal{M}_1 = \sum_n\sum_m\Bigg[&\frac{(\vec{L}_P\cdot\hat{\vec{D}}_{gn})(\vec{L}_1^*\cdot\hat{\vec{D}}_{nm})(\vec{L}_2^*\cdot\hat{\vec{D}}_{mg})}{(\omega_{ng}+\omega_1+\omega_2)(\omega_{mg}+\omega_2)} \\
&+\frac{(\vec{L}_P\cdot\hat{\vec{D}}_{gn})(\vec{L}_2^*\cdot\hat{\vec{D}}_{nm})(\vec{L}_1^*\cdot\hat{\vec{D}}_{mg})}{(\omega_{ng}+\omega_1+\omega_2)(\omega_{mg}+\omega_1)} \\
&+\frac{(\vec{L}_1^*\cdot\hat{\vec{D}}_{gn})(\vec{L}_P\cdot\hat{\vec{D}}_{nm})(\vec{L}_2^*\cdot\hat{\vec{D}}_{mg})}{(\omega_{ng}-\omega_1)(\omega_{mg}+\omega_2)} \\
&+\frac{(\vec{L}_2^*\cdot\hat{\vec{D}}_{gn})(\vec{L}_P\cdot\hat{\vec{D}}_{nm})(\vec{L}_1^*\cdot\hat{\vec{D}}_{mg})}{(\omega_{ng}-\omega_2)(\omega_{mg}+\omega_1)} \\
&+\frac{(\vec{L}_1^*\cdot\hat{\vec{D}}_{gn})(\vec{L}_2^*\cdot\hat{\vec{D}}_{nm})(\vec{L}_P\cdot\hat{\vec{D}}_{mg})}{(\omega_{ng}-\omega_1)(\omega_{mg}-\omega_1-\omega_2)} \\
&+\frac{(\vec{L}_2^*\cdot\hat{\vec{D}}_{gn})(\vec{L}_1^*\cdot\hat{\vec{D}}_{nm})(\vec{L}_P\cdot\hat{\vec{D}}_{mg})}{(\omega_{ng}-\omega_2)(\omega_{mg}-\omega_1-\omega_2)}\Bigg],
\end{aligned}
\tag{13}
$$

where $\vec{L}_j\equiv\vec{L}_{\vec{k}_j s_j}$ $(j=1,2,P)$. For clarity, we omitted in Eq. (13) the usual convergence factor γ; it can be restored by letting $\omega_{ab}\rightarrow\omega_{ab}-i\gamma$. Similarly we obtain the expression of the other amplitudes from Eqs. (11)–(13). It is worthwhile noting that Eq. (13) differs from the one calculated in the case of free space, because vectorial mode functions $\vec{L}_{\vec{k}s}(\vec{x})$ replace usual polarization vectors $\vec{\epsilon}_{\vec{k}s}$.

In order to evaluate the parametric scattering cross section, it is convenient to distinguish the radiation field contribution to the scattering amplitudes $\mathcal{M}_f$ from that of the molecule. Rearranging the indexes in the scalar products in Eq. (13), we can write

$$
\mathcal{M}_f=\sum_i\sum_j\sum_k\epsilon_f^{ijk}\cdot D_{ijk}, \tag{14}
$$

where

$$
\begin{aligned}
D_{ijk} = \sum_n\sum_m\Bigg[&\frac{(\hat{D}_i)_{gn}(\hat{D}_j)_{nm}(\hat{D}_k)_{mg}}{(\omega_{ng}+\omega_1+\omega_2)(\omega_{mg}+\omega_2)} \\
&+\frac{(\hat{D}_i)_{gn}(\hat{D}_k)_{nm}(\hat{D}_j)_{mg}}{(\omega_{ng}+\omega_2+\omega_1)(\omega_{mg}+\omega_1)} \\
&+\frac{(\hat{D}_j)_{gn}(\hat{D}_i)_{nm}(\hat{D}_k)_{mg}}{(\omega_{ng}-\omega_1)(\omega_{mg}+\omega_2)}+\frac{(\hat{D}_k)_{gn}(\hat{D}_i)_{nm}(\hat{D}_j)_{mg}}{(\omega_{ng}-\omega_2)(\omega_{mg}+\omega_1)} \\
&+\frac{(\hat{D}_j)_{gn}(\hat{D}_k)_{nm}(\hat{D}_i)_{mg}}{(\omega_{ng}-\omega_1)(\omega_{mg}-\omega_1-\omega_2)} \\
&+\frac{(\hat{D}_k)_{gn}(\hat{D}_j)_{nm}(\hat{D}_i)_{mg}}{(\omega_{ng}-\omega_2)(\omega_{mg}-\omega_1-\omega_2)}\Bigg].
\end{aligned}
\tag{15}
$$

In the above expression, $\hat{D}_j$ is the jth component of the vectorial operator $\hat{\vec{D}}$. So we define the coherent scattering tensor of the molecule as [18]

$$
\tilde{d}_{ijk}=\frac{e^3}{2\hbar^2}D_{ijk}. \tag{16}
$$

The presence of the cavity is computed by the quantities ϵ_f^{ijk} in Eq. (14):

$$
\begin{aligned}
\epsilon_1^{ijk}(\vec{x}) &= [\vec{L}_{\vec{k}_P s_P}(\vec{x})]^i[\vec{L}^*_{\vec{k}_1 s_1}(\vec{x})]^j[\vec{L}^*_{\vec{k}_2 s_2}(\vec{x})]^k, \\
\epsilon_2^{ijk}(\vec{x}) &= [\vec{L}_{\vec{k}_P s_P}(\vec{x})]^i[\vec{R}^*_{\vec{k}_1 s_1}(\vec{x})]^j[\vec{R}^*_{\vec{k}_2 s_2}(\vec{x})]^k, \\
\epsilon_3^{ijk}(\vec{x}) &= [\vec{L}_{\vec{k}_P s_P}(\vec{x})]^i[\vec{L}^*_{\vec{k}_1 s_1}(\vec{x})]^j[\vec{R}^*_{\vec{k}_2 s_2}(\vec{x})]^k, \\
\epsilon_4^{ijk}(\vec{x}) &= [\vec{L}_{\vec{k}_P s_P}(\vec{x})]^i[\vec{R}^*_{\vec{k}_1 s_2}(\vec{x})]^j[\vec{L}^*_{\vec{k}_2 s_2}(\vec{x})]^k.
\end{aligned}
$$

Now we can write Eq. (12) as

$$
W=\overline{N}_P\,\frac{2\pi\hbar\,\omega_P\omega_1\omega_2}{(2\epsilon_0 V)^3}\left(\sum_{f=1}^{4}|\Delta\epsilon_f(\vec{x})|^2\right)\delta(\omega_P-\omega_1-\omega_2), \tag{17}
$$

where

$$\Delta\epsilon_f(\vec{x}) \equiv 2\sum_i \sum_j \sum_k \epsilon_f^{ijk}(\vec{x})\tilde{d}_{ijk}. \tag{18}$$

Multiplying Eq. (17) by the two-photon final state density of the electromagnetic field ($\propto d^3k_1 d^3k_2$), we obtain the differential scattering transition rate dW for a fixed polarization. We are interested in calculating the differential probability for one of the two photons, for example number 1, independently from its polarization; so we integrate in d^3k_2 and sum over all final polarization states, obtaining

$$d^2W_1(\vec{x}) = \overline{\phi}_P \frac{\hbar\omega_P}{2^8\pi^5 c\epsilon_0^3}\left(\frac{\omega_P-\omega_1}{c}\right)^3\left(\frac{\omega_1}{c}\right)^3 \times\left(\int d\Omega_2 \sum_{\text{pol}} \sum_{f=1}^{4} |\Delta\epsilon_f(\vec{x})|^2\right) d\omega_1 d\Omega_1, \tag{19}$$

where we denote by $\overline{\phi}_P = c\overline{N}_P/V$ the pumping photon flux. We assume the pumping field is not confined by the cavity, and that its wavelength is not included in the mirror reflectivity spectrum; so it is described by a plane wave as in free space:

$$\vec{L}_{\vec{k}_P s_P}(\vec{x}) = \hat{x}\ \exp(i\vec{k}_P\cdot\vec{x}) \tag{20}$$

Now we sum over all final polarization states, Equation (18) becomes $2\Sigma_{jk}\tilde{d}_{xjk}\epsilon_f^{xjk}$ because $(\hat{x})^i = \delta_x^i$. Moreover, many molecules have just one or two nonvanishing nonlinear coefficients, for example, the 2-methyl-4-nitroaniline (MNA) molecule [19] has just $d_{xxx} \equiv d_{11}$ and $d_{xyy} \equiv d_{12}$ nonzero. If we consider an oriented molecule, placed at $\vec{x}$ inside the microcavity and with principal axis (pa) of the index ellipsoid such as $d_{xxx}|_{\text{pa}} \to d_{xxx}|_{\text{cav}}$ and $d_{xyy}|_{\text{pa}} \to d_{xzz}|_{\text{cav}}$, then the sum argument becomes $\tilde{d}_{xjj}\epsilon_f^{xjj}$, where $j = x$ or z. These two cases represent a molecular dipole moment orientation parallel and perpendicular to the mirrors' surfaces respectively. Then Eq. (19) can be divided in two expressions for parallel ($\parallel$) and perpendicular ($\perp$) orientations: We can write

$$\frac{d^2W_1^{\parallel,\perp}}{d\omega_1 d\Omega_1} = \overline{\phi}_P\left(\frac{\mu_0}{\epsilon_0}\right)^{3/2}\frac{\hbar\omega_P(\omega_P-\omega_1)^3\omega_1^3}{2^4\pi^5c^4}\tilde{d}_{1(1,2)}^2\int d\Omega_2 \times\prod_{j=1}^{2}\left[\frac{1}{2}\sum_{s_j}(|\vec{L}_{\vec{k}_j s_j}^{x,z}|^2 + |\vec{R}_{\vec{k}_j s_j}^{x,z}|^2)\right]_{\omega_2=\omega_P-\omega_1}. \tag{21}$$

Note that the expression of the vacuum fluctuations appears in the product in Eq. (21) because, in the parametric process we are considering, we have two frequencies of the field confined by the microcavity. We do not discuss Eq. (21) because its dependence on the microcavity parameters is completely determined by the vacuum fluctuations examined in Sec. III B.

B. Second-harmonic generation

Now consider sum frequency generation processes. We assume that incident fields with frequencies ω_1 and ω_2 are not confined by the cavity, and that they are both in a coherent state with polarization $\hat{x}$ and wave vectors $\vec{k}_1$ and $\vec{k}_2$, respectively. We also assume that the molecular initial state is the ground state, and thus the total initial state is:

$$|\psi_i\rangle = |g\rangle_M \otimes |\phi_1^{\text{inc}}, \phi_2^{\text{inc}}\rangle_F \equiv |g, \phi_i^{\text{inc}}\rangle. \tag{22}$$

The molecular final state is still its ground state, while there are two different final states for the radiation field:

$$\begin{aligned} |\phi_1^{fin}\rangle_F &= \hat{a}_{\vec{k}_3 s_3}^{(L)\dagger}|0\rangle_F |N_1-1, N_2-1\rangle_F, \\ |\phi_2^{fin}\rangle_F &= \hat{a}_{\vec{k}_3 s_3}^{(R)\dagger}|0\rangle_F |N_1-1, N_2-1\rangle_F. \end{aligned} \tag{23}$$

As for the parametric case, the transition rate for a fixed polarization is

$$W = \overline{N}_1\overline{N}_2\frac{2\pi\omega_1\omega_2\omega_3}{\hbar^3}\left(\frac{e^2}{2\epsilon_0 V}\right)^3(|\mathcal{M}_1|^2 + |\mathcal{M}_2|^2) \times\delta(\omega_3-\omega_1-\omega_2), \tag{24}$$

where $\mathcal{M}_f$, $(f=1,2)$ is the same in Eq. (14), where ϵ_f^{ijk} are now

$$\begin{aligned} \epsilon_1^{ijk}(\vec{x}) &= [\vec{L}_{\vec{k}_1 s_1}(\vec{x})]^i[\vec{L}_{\vec{k}_2 s_2}(\vec{x})]^j[\vec{L}_{\vec{k}_3 s_3}^*(\vec{x})]^k, \\ \epsilon_2^{ijk}(\vec{x}) &= [\vec{L}_{\vec{k}_1 s_1}(\vec{x})]^i[\vec{L}_{\vec{k}_2 s_2}(\vec{x})]^j[\vec{R}_{\vec{k}_3 s_3}^*(\vec{x})]^k. \end{aligned} \tag{25}$$

In SFG we only consider the molecular dipole moment parallel to the mirrors' surfaces, so multiplying Eq. (24) for the one-photon final state density ($\propto d^3k_3$) and integrating, we obtain

$$dW_3^{\parallel}(\vec{x}) = \overline{\phi}_1\overline{\phi}_2\frac{\hbar\omega_1\omega_2(\omega_1+\omega_2)^3}{(2\pi c)^2}\left(\frac{\mu_0}{\epsilon_0}\right)^{3/2}\tilde{d}_{11}^2 \times\left[\frac{1}{2}\sum_{s_3}(|\vec{L}_{\vec{k}_3 s_3}^x|^2 + |\vec{R}_{\vec{k}_3 s_3}^x|^2)\right]d\Omega_3, \tag{26}$$

where $\overline{\phi}_j = c\overline{N}_j/V$, $(j=1,2)$ is the incident flux. In SHG, we have

$$\omega_1 = \omega_2 \equiv \omega \Rightarrow \omega_3 = 2\omega.$$

Then, introducing the field intensity $\overline{I}^{\omega} = \overline{\phi}_{\omega}\hbar\omega$ at frequency ω, we can write Eq. (26) as

$$\frac{dW^{\parallel}}{d\Omega}(\vec{x}) = \left(\frac{\mu_0}{\epsilon_0}\right)^{3/2}\frac{2\omega^3\tilde{d}_{11}^2}{\hbar\pi^2c^2}(\overline{I}^{\omega})^2\left[\frac{1}{2}\sum_s[|\vec{L}_{2\vec{k}s}^x|^2 + |\vec{R}_{2\vec{k}s}^x|^2]\right]. \tag{27}$$

This expression contains the vacuum field fluctuations via the expression between square parentheses, like Eq. (21) does. Now in Eq. (27) we have only one field confined by a microcavity, then the vacuum fluctuations appear as single term calculated at the angular frequency 2ω, rather than the product we have obtained in Eq. (21).

IV. VACUUM FIELD FLUCTUATIONS

The role that vacuum field fluctuations play in the SpE process in a microcavity it is well known [3,4]. Now we investigate their effects on nonlinear processes. We have already seen, in Eqs. (21) and (27), how vacuum fluctuations formally appear in parametric processes and SHG; now we calculate these effects explicitly. Then we consider vacuum field fluctuations in a microcavity. If we use $(j=x,y,z)$ to label the electromagnetic field components with respect to the cavity axes, we have

$$\mathcal{V}^j(z)\equiv\langle 0|(\hat{\vec{E}}^j_{\rm cav})^2|0\rangle=\sum_{\vec{k}s}\left(\frac{\hbar ck}{2\epsilon_0 V}\right)[|\vec{L}^j_{\vec{k}s}|^2+|\vec{R}^j_{\vec{k}s}|^2]$$
$$=\frac{\hbar}{8\pi^3\epsilon_0 c^3}\int\omega^3\left[\frac{1}{2}\sum_s[|\vec{L}^j_{\vec{k}s}|^2+|\vec{R}^j_{\vec{k}s}|^2]\right]d\omega\, d\Omega. \tag{28}$$

In Eq. (28) we converted the summation to an integration in the usual way. In this equation we find expressions already seen in Eqs. (21) and (27); let us study the cases of interest to us, i.e., those for $j=x$ and $j=z$. Now we sum over the polarization index s, obtaining for the two cases under examination:

$$\mathcal{V}^{\parallel}(z)\equiv\langle 0|(\hat{\vec{E}}^x_{\rm cav})^2|0\rangle=\frac{\hbar}{8\pi^3\epsilon_0 c^3}\int\omega^3[(\sin^2\phi)N^+_{\vec{k}1}(z)$$
$$+(\cos^2\theta)(\cos^2\phi)N^+_{\vec{k}2}(z)]d\omega\, d\Omega, \tag{29}$$
$$\mathcal{V}^{\perp}(z)\equiv\langle 0|(\hat{\vec{E}}^z_{\rm cav})^2|0\rangle$$
$$=\frac{\hbar}{8\pi^3\epsilon_0 c^3}\int\omega^3[(\sin^2\theta)N^-_{\vec{k}2}(z)]d\omega\, d\Omega,$$

where

$$N^{\pm}_{\vec{k}s}(z)=\tfrac{1}{2}[Q^{(L\pm)}_{\vec{k}s}+Q^{(R\pm)}_{\vec{k}s}] \tag{30}$$

and

$$Q^{(L\pm)}_{\vec{k}s}(z)=(1-|r_{1s}|^2)\,\frac{|1\pm r_{2s}\exp(2iw_-)|^2}{|1-r_{1s}r_{2s}\exp(2iw)|^2}, \tag{31}$$
$$Q^{(R\pm)}_{\vec{k}s}(z)=(1-|r_{2s}|^2)\,\frac{|1\pm r_{1s}\exp(2iw_+)|^2}{|1-r_{1s}r_{2s}\exp(2iw)|^2}$$

and

$$w=kL_c\cos\,\theta, \tag{32}$$
$$w_{\pm}(z)=k\left(\frac{L_c}{2}\pm z\right)\cos\,\theta.$$

Comparing Eqs. (28) and (29), we immediately see that the following relations are strictly valid:

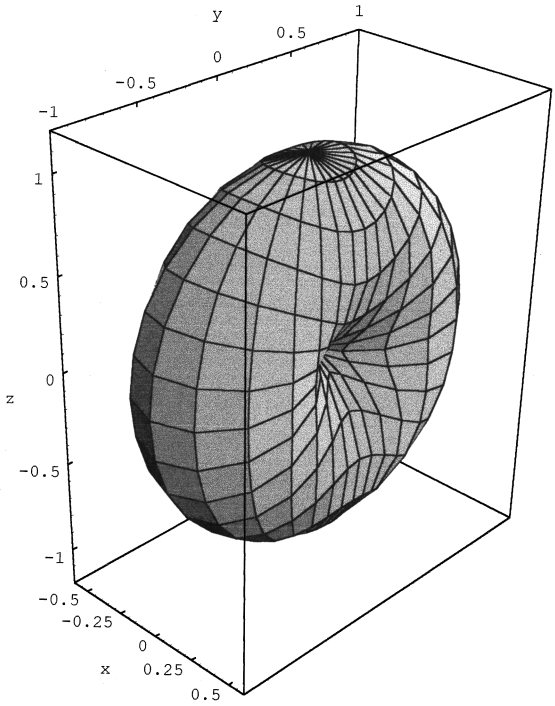

FIG. 4. Polar graph of vacuum field fluctuations of the x component of the electric field (in units of $\hbar\omega^3/8\pi^3\epsilon_0 c^3$) in free space, as functions of the direction (θ,ϕ) of the $\vec{k}$ mode.

$$\frac{1}{2}\sum_s(|\vec{L}^{x,z}_{\vec{k}s}|^2+|\vec{R}^{x,z}_{\vec{k}s}|^2)$$
$$=\left(\frac{\hbar\omega^3}{8\pi^3 c_0 c^3}\right)^{-1}\frac{d^2\mathcal{V}^{\parallel,\perp}}{d\omega\, d\Omega}(z)$$
$$=\begin{cases}(\sin^2\phi)N^+_{\vec{k}1}+(\cos^2\theta)(\cos^2\phi)N^+_{\vec{k}2} & \text{for } \parallel\\ (\sin^2\theta)N^-_{\vec{k}} & \text{for } \perp.\end{cases} \tag{33}$$

Now consider three subcases.

1. Free space

In this case $r_{1s}=r_{2s}=0$ so that $N^{\pm}_{\vec{k}s}(z)=1$, and Eq. (29) leads to one expression valid for all j and independent of spatial coordinates:

$$\mathcal{V}_0\equiv\langle 0|(\hat{\vec{E}}^j_{\rm vacuum})^2|0\rangle=\frac{\hbar}{6\pi^2\epsilon_0 c^3}\int\omega^3 d\omega. \tag{34}$$

Equation (34) is the well-known expression for vacuum field fluctuations in free space [20]; it can be conveniently written as

$$\frac{3}{4\pi}\frac{d\mathcal{V}_0}{d\omega}=\frac{\hbar\omega^3}{8\pi^3\epsilon_0 c^3}. \tag{35}$$

Comparing Eqs. (33) and (35), we deduce

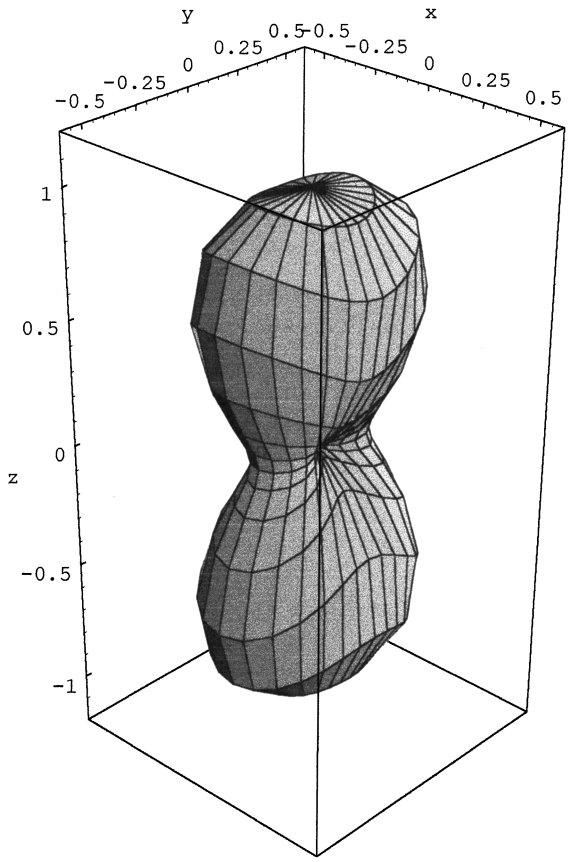

FIG. 5. Polar graph of vacuum field fluctuations normalized at $\theta=0$, of the x component of the electric field (in units of $\hbar\omega^3/8\pi^3\epsilon_0 c^3$), calculated for a molecule placed at the center of a symmetrical cavity with reflectivity $R=0.1$.

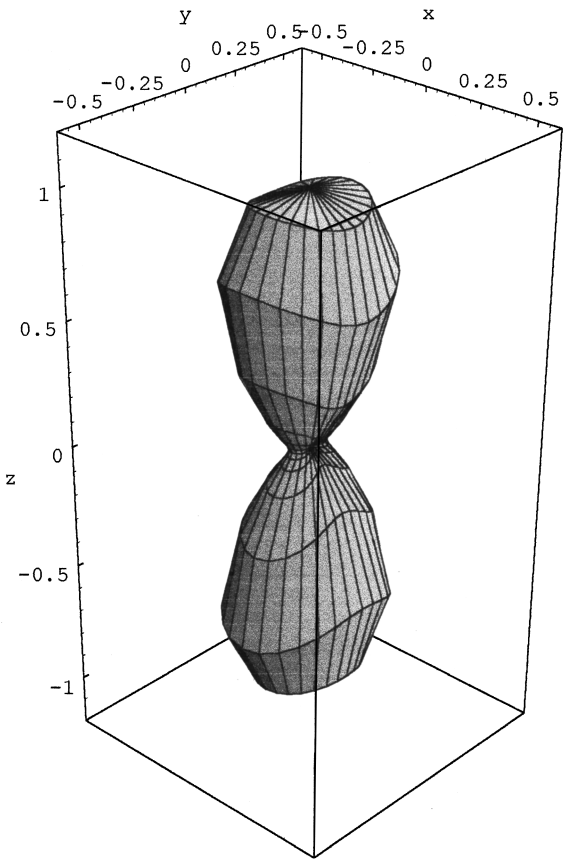

FIG. 6. Polar graph of vacuum field fluctuations, normalized at $\theta=0$, of the x component of the electric field (in units of $\hbar\omega^3/8\pi^3\epsilon_0 c^3$), calculated for a molecule placed at the center of a symmetrical cavity with reflectivity $R=0.3$.

$$\frac{1}{2}\sum_s\left[|\vec{L}^{x,z}_{\vec{k}s}|^2+|\vec{R}^{x,z}_{\vec{k}s}|^2\right]=\frac{4\pi}{3}\frac{d^2\mathcal{V}^{\parallel,\perp}}{d\mathcal{V}_0 d\Omega}. \tag{36}$$

The usefulness of this expression will be shown below. As in Ref. [5], we draw in Fig. 4 Eq. (36) as the surface spanned by a vector whose direction is (θ,ϕ), and whose length gives the vacuum field fluctuations of the x component of the electric field (in units of $\hbar\omega^3/8\pi^3\epsilon_0 c^3$).

2. Symmetrical cavity

In this case we put

$$r_{1s}=r_{2s}\equiv r_s=-|r_s|,\quad t_{1s}=t_{2s}\equiv t_s=i|t_s|,$$

giving

$$S^+_{\vec{k}s}(z)\equiv N^+_{\vec{k}s}(z)=\frac{(1-|r_s|)^2+2|r_s|(\sin^2 w_-+\sin^2 w_+)}{1-|r_s|^2+4(|r_s|^{-2}-1)^{-1}\sin^2 w}, \tag{37}$$

$$S^-_{\vec{k}s}(z)\equiv N^-_{\vec{k}s}(z)=\frac{(1-|r_s|)^2+2|r_s|(\cos^2 w_-+\cos^2 w_+)}{1-|r_s|^2+4(|r_s|^{-2}-1)^{-1}\sin^2 w}.$$

If we put Eq. (37) into Eq. (29), we see that the x fluctuation becomes anisotropic along the z axis. This anisotropy increases with the reflectivity $|r_s|$. The coefficients r_s and t_s depend on angle θ, angular frequency $\omega=ck$, and polarization s [15]. Here we assume, for clarity, that they are independent of θ and polarization; furthermore we suppose that the frequency ω in interest fall in the flat part of the reflectivity spectrum of the mirrors, so we put $|r_s(\omega)|^2\equiv R$ safely. We can draw a polar graph of Eq. (36) for a molecule at the center of the cavity with its dipole moment parallel to the mirrors. Furthermore we assume $kL_c=\pi$; that is, we consider a microcavity whose length is half of the wavelength of the mode with wave vector $\vec{k}$.

The results are shown in Fig. 5 for $R=0.1$ and in Fig. 6 for $R=0.3$. We see that as $R\to 1$, the fluctuations become narrower along the z axis rather than the other direction. For $z\neq 0$ these effects become smaller [5].

3. Asymmetrical cavity

In this case we have

$$r_{1s}=-1,\quad t_{1s}=0,\quad r_{2s}=-|r_s|,\quad t_{2s}=i|t_s|$$

so we obtain

$$N^+_{\vec{k}s}(z)=2A_{\vec{k}s}\sin^2 w_+,$$
$$N^-_{\vec{k}s}(z)=2A_{\vec{k}s}\cos^2 w_+, \tag{38}$$

where we define

$$A_{\vec{k}s}=\frac{1+|r_s|}{1-|r_s|+4(|r_s|^{-1}-1)^{-1}\sin^2 w}. \tag{39}$$

This choice will become clear as we discuss bulk parametric fluorescence.

We can now calculate the differential cross-section $d\sigma(\vec{k}_1)\equiv d\sigma_1$ for the spontaneous emission in a parametric scattering process from a single molecule. The cross section is defined as the ratio of the emission rate of the process to the incident pumping photon flux ϕ_P. Using Eqs. (21) and (36), we can write

$$\frac{d\sigma_1^{\parallel,\perp}}{d\omega_1}=\left(\frac{\mu_0}{\epsilon_0}\right)^{3/2}\frac{\hbar\omega_P(\omega_P-\omega_1)^3\omega_1^3}{3^2\pi^3c^4}\,\tilde{d}^2_{1(1,2)}\left(\frac{d\mathcal{V}_1^{\parallel,\perp}}{d\mathcal{V}_{01}}\right)\left(\frac{d\mathcal{V}_2^{\parallel,\perp}}{d\mathcal{V}_{02}}\right). \tag{40}$$

V. PHASE MATCHING IN SHG FOR A SINGLE MOLECULE

In the case of high-Q cavity, the denominator in Eq. (37) can be expanded in a series of partial fractions, according to the Mittag-Leffler theorem, as

$$\frac{1}{(1-|r_s|^2)^2+4|r_s|^2\sin^2 w}\cong\sum_{m=0}^{N}\frac{1}{4|r_s|^2(w-m\pi)^2+(1-|r_s|^2)^2}, \tag{41}$$

where we denote by N the ''cavity order'' [15], so that

$$L_c=N\,\frac{\lambda_0}{2} \tag{42}$$

where λ_0 is a reference wavelength. Using Eq. (41), we can write Eq. (37) as

$$N^{+}_{\vec{k}s}\cong\sum_{m=0}^{N}\frac{(1-|r_s|^2)[(1-|r_s|^2)^2+2|r_s|(\sin^2 w_+ +\sin^2 w_-)]}{4|r_s|^2(w-m\pi)^2+(1-|r_s|^2)^2}. \tag{43}$$

Consider now the case of a single molecule placed in the middle of the cavity, at $z=0$. It is of interest to study SHG emission on the cavity forward mode; hence in Eq. (43) we take only the term $m=N$, obtaining

$$N^{+}_{\vec{k}s}\cong\frac{\pi}{2|r_s|}\,(1+|r_s|^2-2|r_s|\cos w)[\mathcal{L}_{Ns}(w)], \tag{44}$$

where we denoted by $\mathcal{L}_{Ns}(w)$ the following Lorentzian function with the full width at half maximum equal to $(1-|r_s|^2)/|r_s|$.

$$\mathcal{L}_{Ns}(w)=\frac{1}{\pi}\,\frac{\frac{1-|r_s|^2}{2|r_s|}}{\pi(w-N\pi)^2+\left(\frac{1-|r_s|^2}{2|r_s|}\right)^2}. \tag{45}$$

The $\mathcal{L}_{Ns}(w)$ maxima are determined by the resonance condition $w-N\pi=0$. Using Eq. (32), we can write this condition as

$$(k_z-k_{zN})L_c\equiv\Delta k L_c=0, \tag{46}$$

where

$$k_{zN}\equiv\frac{N\pi}{L_c}. \tag{47}$$

By considerations similar to those we made in Sec. IV, but with the difference that now the frequency in interest is 2ω, we put $|r_s(2\omega)|^2\equiv R$. Then we can write the vacuum field part of Eq. (27), using Eqs. (36) and (37), as

$$\frac{1}{2}\sum_s\,[|\vec{L}^x_{2\vec{k}s}|^2+|\vec{R}^x_{2\vec{k}s}|^2]=G_N(\theta)\mathcal{L}_N(\Delta k)\,\frac{d\mathcal{V}_0}{d\Omega}, \tag{48}$$

where

$$G_N(\theta)\equiv\frac{2\pi^2}{3}\,\frac{1+R-2\sqrt{R}\,\cos[2\pi N(\cos\,\theta)\lambda_0/\lambda]}{\sqrt{R}} \tag{49}$$

and

$$\mathcal{L}_N(\Delta k)=\frac{1}{\pi}\,\frac{\frac{1-R}{2\sqrt{R}}}{[(2k_z-2k_{zN})L_c]^2+\left[\frac{1-R}{2\sqrt{R}}\right]^2}. \tag{50}$$

If we choose L_c so that the harmonic at frequency 2ω is in resonance, i.e., $\lambda_0=\lambda/2$, we have $2w=\pi N\cos\theta$. Then $G_N(\theta)$ dependence on θ is that shown in Fig. 7 for several N and $R=0.999$. For $R\geqslant 0.99$ it is almost independent of R. We see that there is resonance on the forward mode in $z=0$ only for odd N; the next maxima are $(N-1)/2$. For even N, vacuum field fluctuations are forbidden along this direction, but they have $N/2$ maxima for $\theta=\arccos[l/N]$ and odd l. Then the angular dependence of $dW^{\parallel}/d\Omega$ is given by a Lorentzian centered on $\theta=0$. The width θ_0 of the angular distribution of the SHG emission can be obtained from Eq. (46) expanding $\cos\theta$ at $\theta=0$:

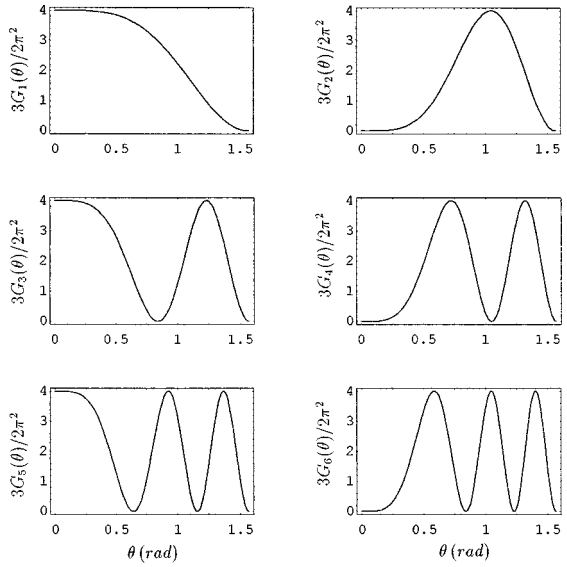

FIG. 7. Plot of $3G_N(\theta)/2\pi^2$ vs θ for several values of N.

$$[2(k_z-k_{zN})L_c]^2\cong\left[\frac{\pi N\theta^2}{2}\right]^2. \tag{51}$$

Setting θ_0 equal to the half width at half maximum (HWHM) of the Lorentzian taken as function of θ^2, we obtain

$$\theta_0\cong\frac{1}{\sqrt{fN}}. \tag{52}$$

In the case of forward mode, Eqs. (49) and (50) become

$$G_N(\theta)\cong\frac{2\pi^2}{3\sqrt{R}}[1-(-1)^N\sqrt{R}]^2\cong\begin{cases}0, & N \text{ even}\\ 8\pi^2/3, & N \text{ odd},\end{cases} \tag{53}$$

$$N\frac{\pi}{2}\mathcal{L}_N(\Delta k)\equiv\mathcal{L}_N(\theta^2)=\frac{1}{\pi}\frac{\frac{1}{fN}}{(\theta^2)^2+\left(\frac{1}{fN}\right)^2}, \tag{54}$$

where $f=\pi\sqrt{R}/(1-R)$ is the cavity finesse [21]. In this limit, we rewrite Eq. (27) as

$$\frac{dP^{2\omega}}{d\cos\theta}=8\left(\frac{\mu_0}{\epsilon_0}\right)^{3/2}\frac{(2\omega)^4\tilde{d}_{11}^2(\bar{I}^{\omega})^2}{3c^2}\frac{\mathcal{L}_N(\theta^2)}{N}, \tag{55}$$

where $P^{2\omega}$ is the emitted power at angular frequency 2ω. The factor $1/N$ comes from the fact that, in the approximations we made, the emitted power is equally distributed among the N resonant modes so that the fraction $1/N$ goes to the forward mode. The Lorentzian function diverges as fN when $\theta\to 0$, but the integration in $d\cos\theta$ gives a factor $d\cos\theta=(\sin\theta)d\theta\simeq\theta_0^2=1/fN$ which compensates for the divergence and assures the energy conservation.

Physically, the divergence angle θ_0 can be related to a finite effective radius r_c of an emitting area parallel to the mirrors' surface, since the divergence is determined by diffraction from a finite area [22]. The relation between the divergence angle θ_0 and the radius r_c of the emitting area parallel to the mirrors' surface can be obtained using diffraction theory or the Heisenberg indetermination principle. These two ways are basically equivalent; indeed, all authors write r_c as

$$r_c=a\lambda_0\sqrt{fN}, \tag{56}$$

where a is an adimensional constant whose value depends on the way followed for the calculation of the formula. Here we use the Heisenberg principle [23]. We assume that the photon moves along the z axis, and hence the uncertainty $\Delta A=\Delta x\Delta y$ on the surface perpendicular to the propagation direction, in which the photon can be localized during the measurement, is

$$\Delta A\simeq\frac{\hbar^2}{\Delta p_x\Delta p_y}. \tag{57}$$

The uncertainty Δp_x on the photon momentum is related to the uncertainty on the corresponding component of the cavity forward mode wave vector $\vec{\bar{k}}$:

$$\Delta p_x=\hbar\Delta(\vec{\bar{k}})_x\equiv\hbar\Delta\bar{k}_x. \tag{58}$$

Similar relations hold for Δp_y and Δp_z. Near the forward mode we can expand at $\theta=0$, and obtain

$$\Delta\bar{k}_x\simeq\bar{k}\sin\theta_0\cong\bar{k}\theta_0, \tag{59}$$

so Eq. (57) becomes

$$\Delta A\simeq\left(\frac{1}{2\pi^2}\lambda_0\sqrt{fN}\right)^2\Rightarrow\Delta x\cong\Delta y\cong 2r_c\cong\frac{1}{2\pi^2}\lambda_0\sqrt{fN}. \tag{60}$$

The uncertainty Δz on the photon longitudinal position is obtained similarly, noting that

$$\Delta\bar{k}_z\cong|\bar{k}(1-\cos\theta)|\cong\bar{k}\frac{\theta_0^2}{2}, \tag{61}$$

from which

$$\Delta z\simeq\frac{1}{\Delta\bar{k}_z}\simeq\frac{4f}{\pi}L_c. \tag{62}$$

It is seen in Eq. (62) that the uncertainty Δz is greater than the cavity geometrical dimension L_c. We note that $4f/\pi$ is approximately the mean number of photon reflections during the photon mean flight time $\tau_c\simeq 2\pi/\Delta\omega$ in the cavity and, therefore, the uncertainty Δz on the photon longitudinal position equals its optical path length inside the cavity. As $\pi/4f$ is also half of the HWHM in Eq. (50) we can introduce the effective length $L_e\equiv\Delta z$, and write Eq. (50) as:

$$\mathcal{L}_N(\Delta k)=\frac{1}{2\pi}\frac{L_e}{L_c}\tilde{\mathcal{L}}_N(\Delta k), \tag{63}$$

where we use a pseudo-Lorentzian $\tilde{\mathcal{L}}_N(\Delta k)$ function defined as

$$\tilde{\mathcal{L}}_N(\Delta k)\equiv\frac{1}{1+(\Delta k L_e/2)^2}. \tag{64}$$

If we denote by $A_c=\pi r_c^2$ the coherence area, and by $V_c=A_c L_e$ the coherence volume, we can define an effective nonlinearity coefficient d_{11} as

$$d_{11}\equiv\frac{\overline{N}_e}{V_c}\,\tilde{d}_{11}, \tag{65}$$

where $\overline{N}_e$ is the effective mean number of emettitors in the cavity. Then it can be easily demonstrated that Eq. (55) becomes

$$\frac{\overline{P^{2\omega}}}{\overline{P^{\omega}}}=\frac{1}{4}\left(\frac{\mu_0}{\epsilon_0}\right)^{3/2}(\omega^2 d_{11}^2 L_e^2)\left(\frac{\overline{P^{\omega}}}{A_c}\right)\tilde{\mathcal{L}}_N(\Delta k) \tag{66}$$

if we write $\overline{N}_e\equiv\sqrt{L_e/L_c}$. Equation (66) is surprisingly similar to the expression of the SHG by a crystal of length L_e pumped by a monochromatic beam of intensity $I^{\omega}=P^{\omega}/A_c$ [12]. A possible interpretation of such similarity follows. Because of reflections inside the volume V_c there is a mean number L_e/L_c of images placed along the z axis at distance L_c between each other. They behave like a crystal of effective length L_e, section area A_c and density $\sqrt{(L_e/L_c)}/V_c$, and assure the quasiconservation of momentum along the z direction. But nonlinearity d_{11} in the expression of the polarization of the ''medium'' created by interference of images cannot be proportional to $\overline{N}_e$, because that would mean counting interference effects twice; hence it must depend only on the square root of this density, so its square is simply equal to the sum of the contributions due to each single image. In conclusion we have shown that, in the presence of a cavity, it is possible to introduce an effective length, similar to the crystal coherence length, even for a pointlike object like an atom or a molecule.

VI. DIFFERENTIAL EXTINCTION COEFFICIENT

Until now we considered a single quantum system in a cavity both in the case of parametric fluorescence and of SHG. In a realistic experiment we should use a dense medium in order to have an appreciable radiation emission. For a cavity resonant in the visible or near-infrared part of the electromagnetic spectrum, we have $0.5\ \mu\text{m}\leqslant L_c\leqslant 50\ \mu\text{m}$, but the coherence length l_c of a crystal, i.e., the maximum crystal length that is useful in producing nonlinear power exceeds this value. Indeed, if we take a typical value of $\lambda=1\ \mu$m and $n(2\omega)-n(\omega)\cong 10^{-2}$, we obtain $l_c\cong 100\ \mu$m for no phase-matched processes. So it would be of no use putting a crystal into a microcavity. Greater emission could be obtained using organic and polymer materials which exhibit very large quadratic optical nonlinearities. For example, a crystal of 2-methyl-4-nitroaniline (MNA) [19] is known to be one of the most efficient organic materials for second-order nonlinear interaction. The reported value for the d_{11} component is $500\pm 25\%$ times the d_{11} coefficient of quartz, viz $d_{11}(\text{MNA})=250\pm 62\times 10^{-12}$ m/V [24]. While in inorganic systems nonlinear phenomena arise from band-structure effects, in organic and polymer systems nonlinear optical responses originate primarily from the π-electron excitations on individual molecular or polymer chain units; each unit can be viewed essentially as an independent source of nonlinear optical response. One can calculate the optical response of a macroscopic condensed assembly like a solid by simply summing these individual responses [25]. Then we still use the theory developed above in the case of a single molecule, with slight changes. For the same reasons a satisfactory experiment can be realized putting a diluted solution ($[C]\sim 10^{-3}M$) ($[C]$=concentration in mol/l=M) of organic molecules inside a cavity, for example between two electrodes at an adequate potential, in order to produce an electric-field-induced alignment of dipolar molecules. Adapting the theory developed in Sec. III for a single molecule to the case of a diluted solution, we can disregard the local-field fluctuations, because in these conditions the number of molecules in a unit volume is at least four orders of magnitude less than in a crystal structure. For example, in a MNA crystal there are four molecules for each unit cell, which corresponds to a density of $\sim 9.23M\gg 10^{-3}M$.

We denote $V_\chi=L_x L_y L_z$ the cavity volume occupied by the solution, and $L_z=L_c$; N_m/V_χ is the number of molecules per unit volume inside the cavity. We also denote by $n_j\equiv n(\omega_j)$ the solvent refraction index at frequency ω_j. In a realistic experiment, we measure the power outgoing from one side of the cavity, which, therefore, can be supposed to be asymmetric. We now define the nonlinear susceptibility tensor as:

$$d_{ijk}\equiv\frac{e^3 N_m/V_\chi}{2\hbar^2}\,D_{ijk}=\frac{N_m}{V_\chi}\,\tilde{d}_{ijk}. \tag{67}$$

In order to avoid complications introduced by the asymmetric boundary conditions (void solvent) on mirror surfaces, we shall suppose that the cavity is embedded in the same solvent present inside the cavity. Then the wave vectors $\vec{k}_\pm$ have the same values inside and outside the cavity. Therefore we can apply the theory of Sec. III to calculate the scattering amplitude. We must sum all such scattering amplitudes over all the medium molecules before squaring and, because the only nonvanishing amplitude for an asymmetric cavity is $\mathcal{M}_2$, we can write

$$\begin{aligned}\mathcal{M}_2&=\sum_i\sum_j\sum_k\epsilon_2^{ijk}(\vec{x})D_{ijk}\\&\to\sum_i\sum_j\sum_k\left(\sum_{\vec{x}}\epsilon_2^{ijk}(\vec{x})\right)D_{ijk}\equiv\mathcal{M}_\chi\end{aligned} \tag{68}$$

and

$$\frac{N_m}{V_\chi}\,s^{ijk}\equiv\sum_{\vec{x}}\epsilon_2^{ijk}(\vec{x})=\frac{N_m}{V_\chi}\int_{V_\chi}d^3x\;c_2^{ijk}(\vec{x}), \tag{69}$$

so we have

$$\mathcal{M}_\chi=\frac{\hbar^2}{e^3}\,\Delta\epsilon_\chi,\quad \Delta\epsilon_\chi\equiv 2\sum_i\sum_j\sum_k s^{ijk}d_{ijk}. \tag{70}$$

We must keep in mind that, because of the presence of the medium, it is necessary to substitute $\epsilon_0\to\epsilon_0\epsilon_r=\epsilon_0 n_r^2$, where

$n_r \equiv n(\omega_r)$. In the examined case, the term ϵ_0^3 in Eq. (17) comes from the product of three fields at angular frequencies ω_1, ω_2, and ω_P; then

$$\epsilon_0^3 \rightarrow \epsilon_0^3 n_1^2 n_2^2 n_P^2. \tag{71}$$

Moreover, we assume the following dispersion relation is valid:

$$\omega n(\omega) - |\vec{k}| c = 0. \tag{72}$$

So we can write the process probability per unit time as

$$w_\chi = \frac{2\pi \overline{N}_P \hbar \omega_P \omega_1 \omega_2}{(2\epsilon_0 V)^3 n_P^2 n_1^2 n_2^2} |\Delta\epsilon_\chi|^2 \delta(\omega_P - \omega_1 - \omega_2). \tag{73}$$

Before going ahead, let us verify that, in the limit of absence of the cavity, Eq. (73) gives results in agreement with those valid in free space. For this purpose we compare our results with those in Ref. [13]. In the free-space limit, we have

$$\epsilon_2^{ijk}(\vec{x}) = (\vec{\epsilon}_{\vec{k}_P s_P})^i (\vec{\epsilon}_{\vec{k}_1 s_1})^j (\vec{\epsilon}_{\vec{k}_2 s_2})^k \exp[i(\vec{k}_P - \vec{k}_1 - \vec{k}_2)\vec{x}] \tag{74}$$

Then, after integration, we obtain

$$\Delta\epsilon_\chi = (2\pi)^2 \left[4\pi \sum_{ijk} d_{ijk} (\vec{\epsilon}_{\vec{k}_P s_P})^i (\vec{\epsilon}_{\vec{k}_1 s_1})^j (\vec{\epsilon}_{\vec{k}_2 s_2})^k \right] \times \delta(\vec{k}_P - \vec{k}_1 - \vec{k}_2), \tag{75}$$

We compare Eq. (75) with Eq. (17) in Ref. [13]: noting that $d_{ijk} = (4\pi\epsilon_0)^{3/2} \chi_{ijk}^{NL}$, if we put

$$(\vec{\epsilon}_{\vec{k}_P s_P})^i (\vec{\epsilon}_{\vec{k}_1 s_1})^j (\vec{\epsilon}_{\vec{k}_2 s_2})^k \rightarrow e_i(\hat{k}_p) o_j(\hat{k}_1) o_k(\hat{k}_2), \tag{76}$$

we find

$$\Delta\epsilon_\chi = (4\pi\epsilon_0)^{3/2} (2\pi)^2 \Delta\epsilon_1 \delta(\vec{k}_P - \vec{k}_1 - \vec{k}_2), \tag{77}$$

where $\Delta\epsilon_1$ is defined in Eq. (17) in Ref. [13]. Furthermore, in Eq. (73), we make the assumptions

$$\begin{aligned} n_P^2 n_1^2 n_2^2 &\rightarrow n_e^2(\vec{k}_p) n_o^2(\vec{k}_1) n_o^2(\vec{k}_2), \\ \omega_P \omega_1 \omega_2 &\rightarrow \omega_{ep} \omega_{o1} \omega_{o2}. \end{aligned} \tag{78}$$

We have identified the dispersive features of the solution with those of the crystal in Ref. [13]. Then the process rate is

$$\frac{w_\chi}{V} = \frac{\overline{N}_P}{V} \frac{(2\pi)^5}{V^2} \frac{(\Delta\epsilon_1)^2 \hbar \omega_{ep} \omega_{o1} \omega_{o2}}{n_e^2(\vec{k}_p) n_o^2(\vec{k}_1) n_o^2(\vec{k}_2)} \delta(\vec{k}_p - \vec{k}_1 - \vec{k}_2) \times \delta(\omega_{ep} - \omega_{o1} - \omega_{o2}). \tag{79}$$

The differential extinction coefficient $d\sigma(\vec{k}_1)$ is obtained dividing Eq. (79) by the incident pump flux $N_p C / n_e(\vec{k}_p) V$ and summing over final states. Since we have considered a monochromatic pump, we can also integrate in $d\vec{k}_p$ after having defined $G(\vec{k}_p) \equiv \delta(\vec{k}_p - \vec{k}_p')$, obtaining

$$d\sigma(\vec{k}_s) = \int\int \frac{(\Delta\epsilon_1)^2 \hbar \omega_{ep} \omega_{os} \omega_{oi} G(\vec{k}_p)}{2\pi C n_e(\vec{k}_p) n_o^2(\vec{k}_s) n_o^2(\vec{k}_i)} \delta(\vec{k}_p - \vec{k}_i - \vec{k}_s) \times \delta(\omega_{ep} - \omega_{oi} - \omega_{os}) d\vec{k}_i d\vec{k}_p d\vec{k}_s, \tag{80}$$

where we renamed the indexes $1 \rightarrow s$ and $2 \rightarrow i$. Equation (80) is exactly the same as Eq. (24) in Ref. [13], confirming that our model is correct. Now we suppose that all molecules are aligned along the x axis, so in the expression of $\Delta\epsilon_\chi$ only one term is nonzero:

$$\Delta\epsilon_\chi = 2 s^{xxx} d_{xxx} \equiv 2 s^{11} d_{11}, \tag{81}$$

where we used the crystallografic notation [12].

After volume integration we find

$$s^{11} = V_\chi \left(\prod_{j=1}^{2} P_{\vec{k}_j s_j} \vec{\epsilon}^{\,x}_{\vec{k}_j s_j} \right) \times \left(\prod_{m=x,y} \frac{\sin[\frac{1}{2}(\vec{k}_P - \vec{k}_1 - \vec{k}_2)_m L_m]}{[\frac{1}{2}(\vec{k}_P - \vec{k}_1 - \vec{k}_2)_m L_m]} \right) Z(\vec{k}_1, \vec{k}_2), \tag{82}$$

where we introduced the function $Z(\vec{k}_1, \vec{k}_2)$:

$$Z(\vec{k}_1, \vec{k}_2) \equiv S_{--} \exp[-i(w_1 + w_2)] - S_{+-} \exp(-i w_1) - S_{-+} \exp(-i w_2) + S_{++} \tag{83}$$

and

$$P_{\vec{k}_j s_j} \equiv \frac{i |t_{s_j}|}{1 - |r_{s_j}| \exp(-2 i w_j)}. \tag{84}$$

We have also defined the following four functions:

$$\begin{aligned} S_{--} &= \frac{\sin[\frac{1}{2}(\vec{k}_P - \vec{k}_1 - \vec{k}_2)_z L_z]}{[\frac{1}{2}(\vec{k}_P - \vec{k}_1 - \vec{k}_2)_z L_z]}, \\ S_{-+} &= \frac{\frac{1}{2}\sin[\frac{1}{2}(\vec{k}_P - \vec{k}_1 + \vec{k}_2)_z L_z}{[\frac{1}{2}(\vec{k}_P - \vec{k}_1 + \vec{k}_2)_z L_z]}, \\ S_{+-} &= \frac{\sin[\frac{1}{2}(\vec{k}_P + \vec{k}_1 - \vec{k}_2)_z L_z]}{[\frac{1}{2}(\vec{k}_P + \vec{k}_1 - \vec{k}_2)_z L_z]}, \\ S_{++} &= \frac{\sin[\frac{1}{2}(\vec{k}_P + \vec{k}_1 + \vec{k}_2)_z L_z]}{[\frac{1}{2}(\vec{k}_P + \vec{k}_1 + \vec{k}_2)_z L_z]}. \end{aligned} \tag{85}$$

In Eq. (73), there is a square absolute value of $\Delta\epsilon_\chi$, and we also have to sum over the final polarization states which appear in Eq. (82) only in the first product; making the

calculation, we find

$$\sum_{\text{pol}} \left| \prod_{j=1}^{2} (P_{\vec{k}_j s_j} \vec{\epsilon}^{x}_{\vec{k}_j s_j}) \right|^2 = \prod_{j=1}^{2} [A_{\vec{k}_j 1} \sin^2\phi_j + A_{\vec{k}_j 2} \cos^2\theta_j \cos^2\phi_j] \equiv \mathcal{F}_c(\vec{k}_1)\mathcal{F}_c(\vec{k}_2), \tag{86}$$

where $A_{\vec{k}_j s_j}$ are defined in Eq. (39). If we compare Eqs. (86) and (33), we recover the influence of the vacuum field fluctuations on the process considered. We can now calculate the differential extinction coefficient, multiplying Eq. (73) by the final state density of the electromagnetic field, then summing over polarization states and dividing by the incident pump flux ϕ_P, and finally dividing by the active volume V_χ. So we find

$$d\sigma_\chi(\vec{k}_1) = \left(\frac{\mu_0}{\epsilon_0}\right)^{3/2} \frac{\hbar\omega_P(\omega_P-\omega_1)^3\omega_1^3 n(\omega_1) n(\omega_P-\omega_1) V_\chi d_{11}^2}{2^6\pi^5 c^4 n(\omega_P)} \mathcal{F}_c(\vec{k}_1)\mathcal{F}_c(\vec{k}_2) \times \int d\Omega_2 |Z(\vec{k}_1,\vec{k}_2)|^2 \prod_{m=x,y} \left(\frac{\sin[\frac{1}{2}(\vec{k}_P-\vec{k}_1-\vec{k}_2)_m L_m]}{[\frac{1}{2}(\vec{k}_P-\vec{k}_1-\vec{k}_2)_m L_m]} \right)^2 d\omega_1 d\Omega_1 . \tag{87}$$

A straightforward calculation shows the validity of the following relation:

$$\begin{aligned} |Z(\vec{k}_1,\vec{k}_2)|^2 \equiv & (S_{--}^2 + S_{-+}^2 + S_{+-}^2 + S_{++}^2) \\ & - 2\cos w_1 (S_{++}S_{+-} + S_{--}S_{-+}) \\ & - 2\cos w_2 (S_{++}S_{-+} + S_{--}S_{+-}) \\ & + 2\cos(w_1 - w_2) S_{+-}S_{-+} \\ & + 2\cos(w_1 + w_2) S_{++}S_{--} . \end{aligned} \tag{88}$$

This expression seems complicated; however, all the terms but the first are almost zero, because they are the products of sinc functions [sinc denote $(\sin x)/x$] with different arguments. In the case of near degeneration, $\omega_1 \simeq \omega_2 \simeq \omega_P/2$, and for near-collinear phase matching on the forward mode the only nonzero term is S_{--}. Because L_x and L_y are typically several thousand optical wavelengths, the sinc's product in Eq. (87) can be well approximated by a δ function; that is, we consider the case of cavity mirrors infinitely extended in the x-y plane. If we denote the wave vector $\vec{k}$ by

$$\vec{k} = (\xi\hat{x} + \eta\hat{y}) + \zeta\hat{z} \equiv \vec{k}^{\parallel} + \vec{k}^{\perp}, \tag{89}$$

we can rewrite Eq. (87), after integration in $d\vec{k}_2^{\parallel}$, as

$$d\sigma_\chi(\vec{k}_1) = \frac{\hbar\omega_P\omega_1^3\omega_2 n_1 L_c d_{11}^2}{2^4 c^4 \pi^3 \epsilon_0^3 n_P [n(\omega_P-\omega 1)]^2} \times |Z(\vec{k}_1,\vec{k}_2)|^2 \mathcal{F}_c(\vec{k}_1)\mathcal{F}_c(\vec{k}_2) \frac{\omega_P-\omega_1}{\overline{\zeta}_2} \times \left[\frac{n(\omega_P-\omega_1)}{c}\right]^2 \delta(\zeta_2 - \overline{\zeta}_2) d\zeta_2 d\omega_1 d\Omega_1 , \tag{90}$$

where

$$\overline{\zeta}_2 \equiv \left[\left(\frac{\omega_P-\omega_1}{c} n(\omega_P-\omega_1) \right)^2 - \frac{1}{c^2} (|\vec{k}_P^{\parallel}|^2 + |\vec{k}_1^{\parallel}|^2 - 2\vec{k}_P^{\parallel}\cdot\vec{k}_1^{\parallel}) \right]^{1/2}. \tag{91}$$

We are interested in the possibility of a practical realization of a parametric oscillator in a microcavity, so we suppose that the cavity is resonant on $\vec{k}_1$. In this arrangement $\vec{k}_1^{\parallel} = \vec{0}$, and Eq. (91) becomes simpler. The condition for the argument of the root in Eq. (91) to be positive implies, for $\vec{k}_1^{\parallel} = 0$, a limited set of values for ω_1 as a function of θ_P. Some calculations show that the pump incident angle is limited to

$$0 \leqslant \sin\theta_P \leqslant \frac{n(\omega_P-\omega_1)}{n(\omega_P)} \left(1 - \frac{\omega_1}{\omega_P}\right). \tag{92}$$

Figure 8 shows $\overline{\zeta}_2$ as a function of θ_P and ω_1; the plane part in the graph corresponds to the values forbidden by Eq. (92). It is calculated for a generic medium with a refractive index following Sellmeir's formula [26]. We deduce from it, for example, that the pump incident angle on the microcavity cannot be greater than the value $(\theta_P)_{\text{MAX}} \simeq .31$ if we want to work in conditions of nearly degeneration, i.e., $\omega_1 = \omega_P/2$. Assume now, as in Sec. IV, that mirror reflection and transmission coefficients are independent of polarization and frequency, so we define $|r_s(\omega_1)|^2 \equiv R$. If we set

$$\overline{\vec{k}}_2 \equiv \vec{k}_P^{\parallel} + \overline{\vec{k}_2^{\perp}} = \eta_P\hat{y} + \overline{\zeta}_2\hat{z}, \tag{93}$$

then the differential extinction coefficient becomes

$$d\sigma_\chi(\vec{k}_1) = \frac{(\hbar\omega_P)\omega_1^3(\omega_P-\omega_1)^2 n_1 L_c d_{11}^2}{2^4\pi^3 c^3 n_P \overline{\zeta}_2} \left(\frac{\mu_0}{\epsilon_0}\right)^{3/2} \times |Z(\vec{k}_1,\overline{\vec{k}_2})|^2 \mathcal{F}_c(\vec{k}_1)\mathcal{F}_c(\overline{\vec{k}_2}) d\omega_1 d\Omega_1 . \tag{94}$$

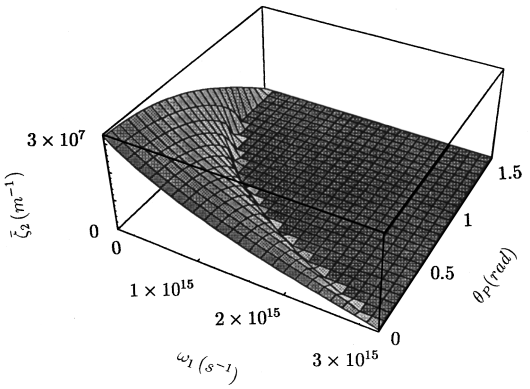

FIG. 8. Graphical representation of allowed values of ω_1 and θ_P, for a generic medium with a refractive index that follows the Sellmeir formula. The plane part of the graph corresponds to the forbidden value.

This formula is the goal of this section. Now we see how it depends on the microcavity parameters. A calculation shows that

$$\mathcal{F}_c(\vec{k}_1)\mathcal{F}_c(\vec{k}_2)=\frac{(1+\sqrt{R})^2}{1+R-2\sqrt{R}\,\cos\left(2\pi N\,\dfrac{\zeta_2}{k_1}\right)}. \quad (95)$$

As in Sec. V, one can demonstrate that in proximity to the mth resonance (m is an integer or zero), $(\zeta_2)_m=k_1 m/N$, and for $1-R\ll 1$, Eq. (95) is well approximated by

$$\mathcal{F}_c(\vec{k}_1)\mathcal{F}_c(\vec{k}_2)\cong f\,\frac{\dfrac{1}{4\pi f}}{(\pi N\zeta_2/k_1-m\pi)^2+\left(\dfrac{1}{4f}\right)^2}. \quad (96)$$

So we can write the energy emitted per unit time in a microcavity $P(\vec{k}_1)$ as

$$P(\vec{k}_1)d\omega_1 d\Omega_1\equiv d\sigma_\chi(\vec{k}_1)\hbar\omega_1 V_\chi\phi_P. \quad (97)$$

If we want to calculate the energy emitted in a microcavity during a process, we must be very careful. We must integrate Eq. (97) over a time interval which depends on the ratio of two parameters: the coherence time of the pumping laser $\tau_P=1/\Delta\nu_P$ and the photon mean flight time in microcavity τ_c. Indeed, because the energy reservoir of the nonlinear phenomena we considered is the pumping laser itself, for $\tau_P/\tau_c<1$ we must integrate between $t=0$ and $t=\tau_P$, but for $\tau_P/\tau_c>1$ the effect of the cavity on the process, that is the validity of Eq. (97), persists only during a time τ_c. Therefore the integration interval is now $0\leqslant t\leqslant\tau_c$. Typically τ_c is of the order of some picoseconds, so the first regime is realized only using ultrashort laser pulses.

Let us briefly discuss the form of Eq. (94): the first factor is simply a number dependent on the examined process and containing the constraint (92) via ζ_2. The function $|Z|^2$ is similar to that of free space $[\mathrm{sinc}(\Delta kL/2)]^2$, made more complicated by the terms due to multiple reflections in the cavity. However, these terms tend to eliminate each other and make a negligible contribution, as we can see in Eq. (88). We note that in conditions of exact resonance, Eq. (95) reduces to $[(1+\sqrt{R})/(1-\sqrt{R})]^2$. This factor, increasing when $R\to 1$, suggests the real possibility of making a microscopic parametric oscillator. Indeed, as the energy of the process is conserved, the increase of power emitted on the forward mode must occur at the expense of other loss channels represented by all the other electromagnetic field modes in the cavity. Then, as happens in a microlaser, we can expect a lower-energy threshold and a gain increase. However, the dynamics of nonlinear processes in microcavities will be treated in a forthcoming work.

VII. SUMMARY

In this work, scattering amplitudes for parametric fluorescence, and SHG emission from a single molecule inside a microcavity, have been computed. We have explicitly written out their dependence on vacuum field fluctuations which have been calculated for several cavity configurations. We have seen that in general vacuum field fluctuations factorize out for fields at angular frequencies ω_1 and ω_2. Concerning SHG from a single molecule, we have shown that in a planar microcavity it is possible to introduce a parameter proportional to the cavity's finesse and length: the effective length L_e, that is analogous to coherence length l_c of a crystal. This is possible because the phase-matching condition, that is the momentum conservation for the electromagnetic field, is assured by the cavity rather than the crystal. In Sec. VI of this paper, we have concentrated on parametric fluorescence from a uniform distribution of aligned dipoles into an asymmetric cavity. The differential extinction coefficient has been calculated, and its dependence on the cavity's parameters discussed; moreover, we have shown that it increases on the forward mode with finesse. This suggests, in analogy with microlaser devices, the possibility of making a microscopic parametric oscillator. Moreover, parametric fluorescence in a microcavity exhibits an interesting behavior with respect to a microlaser. For the parametric fluorescence emission power on the forward mode described in Eq. (97), we have found a ''quadratic'' efficiency [Eq. (96)] which is larger than the corresponding ''linear'' efficiency in microlasers, where only a unique field frequency is confined by the microcavity.

ACKNOWLEDGMENTS

One of the authors (A.A.) is deeply indebted to Professor P. Mataloni for helpful and stimulating discussions, and to Dr. G. D'Auria for reading the manuscript.

[1] S. Haroche and D. Kleppner, Phys. Today **1** (1), 24 (1989).
[2] L. Knöll and D. G. Welsch, Prog. Quantum Electron. **16**, 135 (1992).
[3] *Spontaneous Emission and Laser Oscillation in Microcavities*, edited by H. Yokoyama and K. Ujiara (CRC, Boca Raton, FL, 1995).
[4] F. De Martini, G. Innocenti, G. R. Jacobovitz, and P. Mataloni, Phys. Rev. Lett. **59**, 2955 (1987).
[5] S. M. Dutra and P. L. Knight, Phys. Rev. A **53**, 3587 (1996).
[6] F. De Martini and M. Giangrasso, Appl. Phys. B: Photophys. Laser Chem. **60**, S-49 (1995).
[7] A. Aiello, F. De Martini, M. Giangrasso, and P. Mataloni, Quantum Semiclassic. Opt. **7**, 677 (1995).
[8] F. De Martini, F. Cairo, P. Mataloni, and F. Verzegnassi, Phys. Rev. A **46**, 4220 (1992).
[9] P. Mataloni, A. Aiello, D. Murra, and F. De Martini, Appl. Phys. Lett. **65**, 1891 (1994).
[10] F. Cairo, F. De Martini, and D. Murra, Phys. Rev. Lett. **70**, 1413 (1993).
[11] F. De Martini, M. Marrocco, C. Pastina, and F. Viti, Phys. Rev. A **53**, 471 (1996).
[12] A. Yariv, *Quantum Electronics*, 3rd ed. (Wiley, New York, 1989), Chaps. 16 and 17.
[13] T. G. Giallorenzi and C. L. Tang, Phys. Rev. **166**, 225 (1968).
[14] A. Yariv, IEEE J. Quantum Electron. **QE-13**, 943 (1977).
[15] F. De Martini, M. Marrocco, P. Mataloni, L. Crescentini, and R. Loudon, Phys. Rev. A **43**, 2480 (1991).
[16] M. Ley and R. Loudon, J. Mod. Opt. **34**, 227 (1987).
[17] R. Loudon, *The Quantum Theory of Light*, 2nd ed. (Oxford University Press, Oxford, 1990).
[18] L. D. Landau and E. M. Lifšits, *Teoria Quantistica Relativistica* (Editori Riuniti, Rome, 1978), Chap. VI.
[19] B. F. Levine, C. G. Bethea, C. D. Thurmod, R. T. Lynch, and J. L. Bernstein, J. Appl. Phys. **50**, 2523 (1979).
[20] H. Khrosavi and R. Loudon, Proc. R. Soc. London, Ser. A **433**, 337 (1991).
[21] M. Born and E. Wolf, *Principles of Optics*, 6th ed. (Pergamon, Oxford, 1993).
[22] G. Björk, H. Heitman, and Y. Yamamoto, Phys. Rev. A **47**, 4451 (1993).
[23] F. De Martini, M. Marrocco, and D. Murra, Phys. Rev. Lett. **65**, 1853 (1990).
[24] G. F. Lipscomb, A. F. Garito, and R. S. Narang, J. Chem. Phys. **75**, 1509 (1981).
[25] A. Garito, R. F. Shi, and M. Wu, Phys. Today **57** (5), 51 (1994).
[26] R. Morita, N. Ogasawara, S. Umegaki, and R. Iro, Jpn. J. Appl. Phys. **26**, L1711 (1987).